Academia Journal of Scientific Research 3(3): 000-000, September 2019
DOI: 10.15413/ajsr.2018.2010
ISSN 2315-7712

Author should effect the correction in the references section

Research Paper

Preparation of polyethylene oxide-cobalt hydroxide hybrid nanofibers

Accepted

Mohammad Madani[1,2]*, Ahmad Hasan-Kaviar[3], Abbass Kazemi[4] and Abdelmagid Salem Hamouda[2]

[1]Microbial Biotechnology Department, Agricultural Biotechnology Research Institute of Iran (ABRII), Agricultural Research, Education, and Extension Organization (AREEO), Karaj, Iran.
[2]Department of Mechanical and Industrial Engineering, Qatar University, Doha, Qatar.
[3]School of Chemistry, University College of Science, University of Tehran, Tehran, Iran.
[4]Nanotechnology Research Center, Research Institute of Petroleum Industry (RIPI), Tehran, P. O. Box: 14665-1998, Iran.

*Corresponding author. E-mail: mmadani@khayam.ut.ac.ir.

ABSTRACT

Cobalt hydroxide nanoparticles-polyethylene oxide nanofibers, as organic-inorganic hybrid, were prepared via *in-situ* electrospinning. Thus, electrospinning of polyethylene oxide solution with different cobalt nitrate concentrations was carried out in gaseous ammonia atmosphere. The reaction of cobalt nitrate with ammonia produced cobalt hydroxide. The reaction occurred during fibres formation. Transmission Electron Microscopy (TEM) showed that cobalt hydroxide $Co(OH)_2$ nanoparticles were formed on the produced nanofibers of 100-600 nm in diameter. The existence of the formed $Co(OH)_2$ was also proven by X-ray Diffraction (XRD) analysis and it showed that the $Co(OH)_2$ nanoparticles were produced. Differential Scanning Calorimetry (DSC) analysis was used to determine the melting point and to calculate the crystallinity of the produced hybrid nanofibers. The DSC and Thermogravimetric Analysis (TGA) results of the obtained nanofibers were compared with those of the electrospinning of a polyethylene oxide solution having Co^{+2} ions and a pure polyethylene oxide solution in an air atmosphere. TGA also confirmed the presence of $Co(OH)_2$ within the fibers.

Key words: *In-situ* electrospinning, polyethylene oxide, cobalt hydroxide, nanocomposite.

INTRODUCTION

Cobalt hydroxide or cobaltous hydroxide or cobaltous hydrate, has attracted increasing attention in recent years because of its novel electric and catalytic properties and important technological applications (Xu and Zeng, 1999; Cao et al., 2004; Zhang et al., 2000), for examples in advanced batteries (Elumalai et al., 2001), supercapacitors (Srinivasan and Weidner, 2002), solar cells (Barrera et al., 1998), electrochromics (Kadam et al., 2001), as an oil additive, it can improve tribological properties (Chen et al., 2001), etc.

Several chemical and electrochemical methods have been employed to prepare cobalt hydroxide, for example, direct precipitation with liquid ammonia (Ramesh et al., 2003).

Although many attempts have been made on the synthesis of cobalt hydroxides, the control of their morphology, size, and crystallinity still remains a highly sophisticated challenge to materials scientists and chemists. Therefore, this study also demonstrate a way for the synthesis of $Co(OH)_2$ nanoparticles via electrospinning.

Polymer nanocomposites containing inorganic particles have attracted a great deal of interest from researchers because they frequently exhibit unexpected hybrid properties, synergically derived from both components (Maity and Biswas, 2004). Enhanced conductivity and special mechanical, electrochemical, optical, magnetic as well as thermal properties of these composites make them promising materials.

In the past decade, electrospinning has attracted tremendous interest in the research community. Nanowebs produced by the electrospinning technique have several remarkable functional characteristics such as a very large surface area to volume ratio, pore size within the nano range, unique physical and mechanical properties along with the design flexibility for chemical/physical surface functionalization. This procedure can produce functional nanofibers having optical, electrical, or catalytic properties by incorporating inorganic nanoparticles into the nanofibers. Most of the reported manufacturing methods of polymer-inorganic composite nanofibers are based on electrospinning of polymer solution blended with inorganic nanoparticles (Yang et al., 2003; Yang et al., 2005). Another method of preparing polymeric-inorganic composite nanofibers is based on electrospinning of a polymer precursor having metal ions and the subsequently post-treatment of the produced nanofibers (Lee et al., 2006; Khatri et al., 2013).

The aim of this study was to manufacture organic-inorganic nanofiber hybrids through *in-situ* electrospinning and also to show the possibility of the reaction occurring on the traveling polymer jet in electrospinning within an active atmosphere. Thus, we are reporting *in-situ* synthesis of cobalt hydroxide nanoparticles on polyethylene oxide nanofibers through electrospinning. Extensive characterization of nanofibers was carried out using transmission electron microscopy (TEM), X-ray diffraction (XRD), differential scanning calorimetery (DSC) and thermogravimetric analysis (TGA) techniques and the results were compared with those of the nanofibers produced using electrospinning of the polyethylene oxide solution having Co^{+2} ions and pure polyethylene oxide solution.

EXPERIMENTAL

$Co(NO_3)_2.6H_2O$ (supplied by Merck Chemical Co.) with different concentrations (given in Table 1) was dissolved in 100 mL distilled water to produce Co^{+2} solution. Thereafter, the following seven experiments (Exp. G1, G2, G3, G4, G5 (collectively called G-series in this article), P, and N) were carried out. G-series: 4.0 g of polyethylene oxide (with weight average molecular weight of 600,000 g/mol and supplied by Acros Organics Co.) was added to 100 mL of the above mentioned cobalt nitrate solution with different concentrations (given in Table 1) and left for two nights to obtain a homogenous PEO solution having cobalt ions. The polymer solution was put into a hypodermic syringe. A syringe pump (Stoelting Co., USA) was used to feed the polymer solution into a metallic needle with an inner diameter of 0.7 mm. A grounded aluminum foil as collector was placed at a fixed distance of 18 cm from the needle. The metallic needle and the collector were enclosed in a polymethyl metacrylate box (40×50×60 cm). The feed rate of the syringe pump was fixed at 0.7 mL/h. A positive potential of 18 kV was then applied to the polymer solution using a high-voltage power supplier (HV35P series, Fnm Co., IR) with a maximum voltage of 35 kV. During electrospinning, gaseous ammonia (from a cylinder purchased from Merck Chemical) was purged into the box with a rate of 10 L/min. Electrospun nanofibers were collected on the surface of the grounded aluminum foil.

To compare between the electrospinning of the above-mentioned polyethylene oxide solution having Co^{+2} and pure polyethylene oxide solution, Exp. P and N, respectively were also carried out in air in a way similar to G-series Exp. excluding the box.

A CEM 902A ZEISS Transmission Electron Microscope (TEM) with an accelerating voltage of 80 kV was used to obtain more information about the morphology of fibers and to confirm the presence of $Co(OH)_2$ nanoparticles. The electrospun fibers were directly deposited onto a copper grid and then analyzed using TEM technique.

Thermal properties of the electrospun fibers were analyzed by thermogravimetry (Model TGAQ50, TA Instruments) at 20ºC/min for heating rate and Differential Scanning Calorimetry (Model DSCQ100, TA Instruments) at 10ºC/min for heating rate under the inert gas of Ar.

X-ray diffraction (XRD) patterns of the samples were recorded by an Expert Philips diffractometer with a CuKα anode; scans were made from 10° to 40° (2θ). The nanofiber mats were deposited on a glass during electrospinning and then analyzed using X-ray diffraction method.

RESULTS AND DISCUSSION

A comparison of the appearance (color change) of the mats obtained from G-series with that of the P fiber mat suggested that the cobalt ions in the jet traveling the distance between the needle and the collector could precipitate in the gaseous ammonia atmosphere to produce cobalt hydroxide. In other words, in this process, one reaction occurs during fiber formation: the reaction of Co^{+2} ions with NH_3 which produces $Co(OH)_2$ nanoparticles on the nanofibers.

Cobalt (II) hydroxide is obtained as a precipitate when an alkaline hydroxide is added to an aqueous solution of cobalt (II) salt (Patnaik, 2002). Since the reaction of nanoparticle formations occurs during fiber formation in electrospinning process, the precipitated nanoparticles have special morphology and crystalline structures (due to the applied voltage, elongation, etc.).

Figure 1 shows the TEM images of fibers obtained from Exp. G1 (electrospinning of polyethylene oxide solution having 2.5% Co^{+2} based on PEO, in ammonia atmosphere) and as it shows, dark spots of $Co(OH)_2$ are heterogeneously dispersed on the fibers. Figure 2 shows the TEM images of fibers produced in Exp. G2 (electrospinning of polyethylene oxide solution having 5% Co^{+2} based on PEO, in ammonia atmosphere). These TEM images (Figures 1 and 2) suggest that in the Exp. G1, $Co(OH)_2$ nanoparticles were heterogeneously synthesized on fibers through the reaction of cobalt ions with NH_3 and in Exp. G2, a greater number of $Co(OH)_2$ nanoparticles are formed on the nanofibers through *in situ* chemical reactions during electrospinning due to the higher concentration of the $Co(NO_3)_2$ within the starting solution. In G-series experiments, $Co(OH)_2$ particles

Table 1: Recipes for the electrospinning methods.

Exp.	$Co(NO_3)_2.6H_2O$ (g)	Co^{+2} ions percentage within solution base on PEO (%)	PEO (g)	Atmosphere
G1	0.5	2.5	4	NH3
G2	1	5.0	4	NH3
G3	2	10.0	4	NH3
G4	3	15.0	4	NH3
G5	4	20.0	4	NH3
P	0.5	2.5	4	Air
N	0	0	4	Air

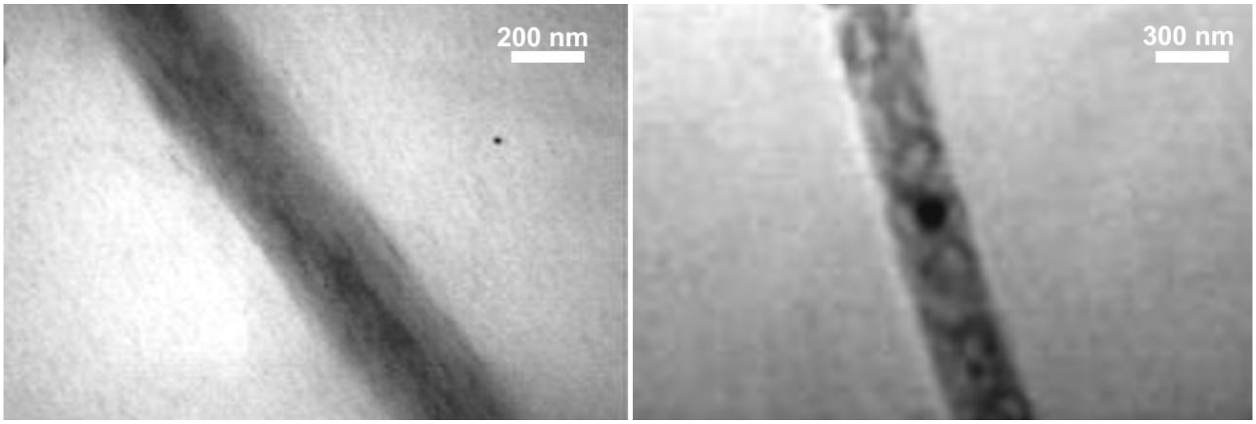

Figure 1: TEM images of nanofibers obtained from Exp. G1.

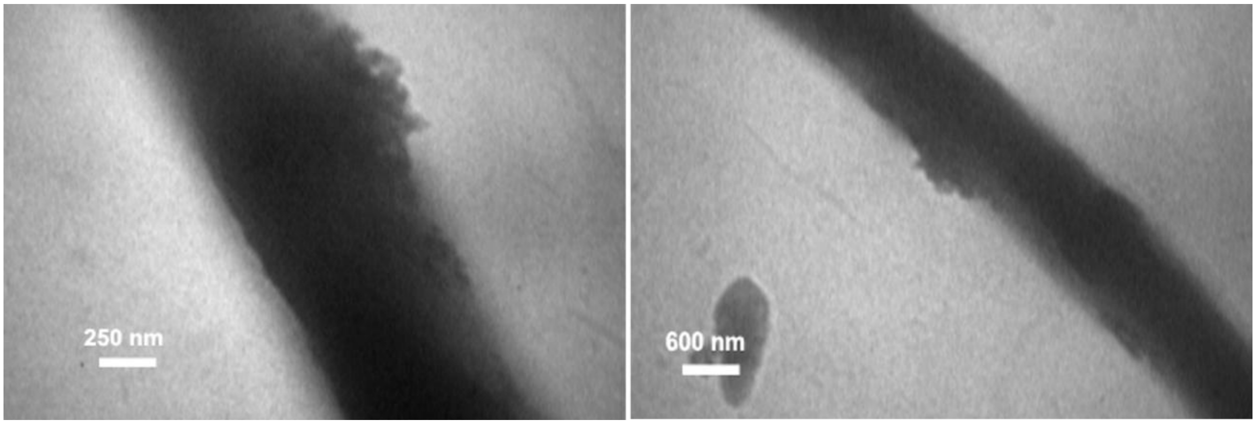

Figure 2: TEM images of nanofibers obtained from Exp. G2.

aggregate to form nanoparticles on the fibers probably due to the insignificant interaction of $Co(OH)_2$ with PEO. This causes $Co(OH)_2$ nanoparticles in G-series experiences to randomly form on the fibers.

The TGA and DTGA thermograms for the pure PEO fibers and their nanocomposites are shown in Figure 4. The curves a, b, c, d, and e, in Figure 3, are TGA thermographs of fiber mats obtained in experiments G4, G3, G2, P, and N, respectively. The initial degradation temperature (T_{onset}), and the thermal decomposition temperature (T_d, obtained by the first derivative of TGA curves) for pure PEO fibers and their composite fibers are summarized in Table 2.

The gradual mass loss in the range of 25–150°C can be attributed to evaporation of the water in the nanofibers. The second step weight loss at 168°C which was not observed in the TGA thermographs of Exp. P and N is due to the decomposition of the cobalt hydroxide to cobalt oxide. The major weight-loss profile exhibits a well-defined

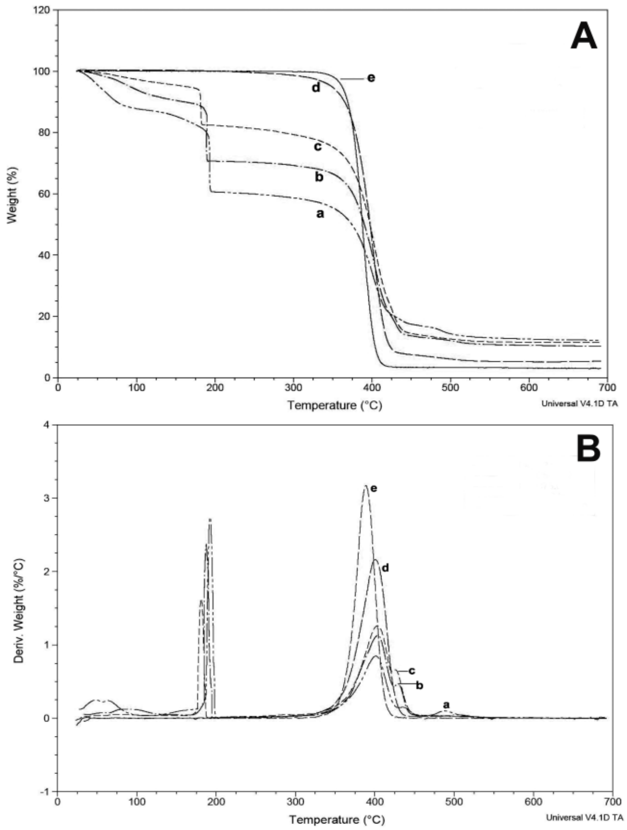

Figure 3: TGA and DTGA thermographs of G4 (a), G3 (b), G2 (c), P (d), and N (e) fibers.

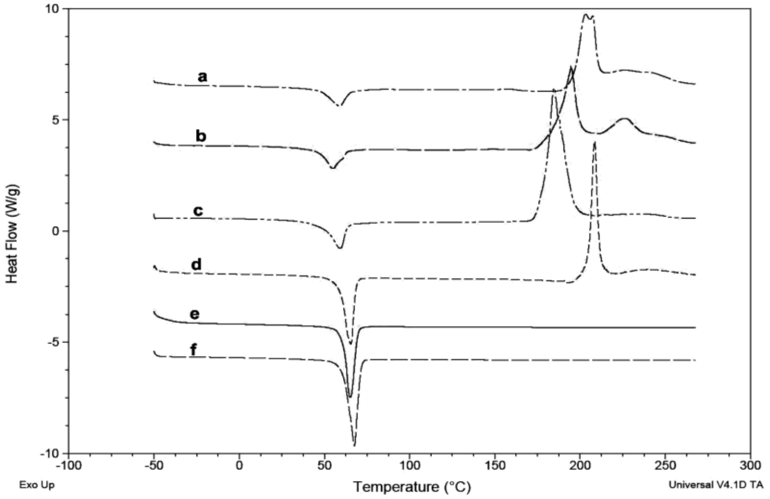

Figure 4: DSC thermographs of G4 (a), G3 (b), G2 (c), G1 (d), P (e), and N (f) fibers.

decrease between 320 and 450°C related to PEO decomposition.

The weight loss measured in the range of 170-260°C is due to the decomposition of Cobalt (II) hydroxide to cobalt(II) oxide. Cobalt oxide can be obtained by a thermal-decomposition method with cobalt hydroxide as the precursor. So, after 260°C in TGA, cobalt hydroxide-PEO nanocomposite is converted to cobalt oxide-PEO

Table 2: Thermal decomposition temperatures and residue of the products obtained from the TGA analyses.

Sample	T_d $Co(OH)_2$ (°C)	$T_{onset}PEO$ (°C)	T_d PEO (°C)	Losing weight between 150-220°C (%)	Residue at 600°C (%)
G4	192	315	401	25.03	13.39
G3	188	332	402	19.92	10.52
G2	180	335	403	13.44	11.40
P	---	320	400	0.84	4.69
N	---	342	388	0.01	3.11

Table 3: The melting points (T_m) and the percentage of crystallinity (X_C %) of the products obtained from the DSC analyses.

Sample	Heating T_m (°C)	Enthalpy of fusion ΔH_{total} (J/g)	Crystallinity %
G4	47.7	45.2	25.8
G3	47.3	52.0	27.6
G2	49.8	64.8	32.2
G1	59.4	115.8	55
P	61.2	112.7	54
N	61.5	148.9	69

nanocomposite.

The comparison of curves a to c with curves d and e shows that the presence of $Co(OH)_2$ nanoparticles in fibers that are converted to cobalt oxide increase the thermal properties of polyethylene oxide fibers from 388°C for pure PEO fibers to 401°C for G4 fibers, but T_{onset} of G fibers become lower than that of N fibers. The T_{onset} of the composites decrease as compared to the pure PEO as the amount of $Co(OH)_2$ increases in the matrix, but due to some factors such as aggregation of $Co(OH)_2$ nanoparticles, there is no linear relationship between $Co(OH)_2$ amounts within the fibers and T_{onset} of composite fibers.

Thermal properties of the fiber mats produced in the experiments (Exp. G1, G2, G3, G4, P, and N) were also analyzed by DSC analysis. The DSC thermographs of the experiments are shown in Figure 4 and the curves a, b, c, d, e and f in this figure are DSC thermographs of fiber mats obtained in experiments G4, G3, G2, G1, P, and N, respectively. The melting points (T_m) and the percentage of crystallinity (X_C %) of the products in the experiments were obtained from the DSC analyses and are listed in Table 3.

The presence of an intense melting peak in the DSC thermographs indicates the semicrystalline products. This figure shows that the melting point of the G-series fibers in curves a to d is lower than that of P fibers. The specific heat of crystallization of the nanocomposite ΔH_{comp} was calculated using the following formula:

$$\Delta H_{comp} = [\Delta H_{total} \times 100] / y$$

where ΔH_{total} is obtained from the peak area of the DSC curve (j/g), and y is the concentration of PEO (wt %). The given crystallinities (X_C %) of the fiber mats in Table 3 were calculated using the equation $X_C \% = [\Delta H_{comp} / \Delta H^{o}_{f}] \times 100$, where ΔH^{o}_{f} is the heat of fusion of completely crystalline polyethylene oxide (that is 213.7 J/g) (Xi and Tang, 2004) and ΔH_{comp} is the heat of fusion for the sample calculated from the former equation. As shown in Figure 5 and Table 3, the melting point and the crystallinity of pure PEO fibers (Exp. N) are higher than those of PEO fibers having $Co(OH)_2$ nanoparticles within them.

The data given in Table 3 also show that the crystallinity and melting point of the fibers produced in Exp. P are higher than those in G-series. This is a result of the presence of $Co(OH)_2$ nanoparticles in fibers produced in G-series.

To confirm the identity of the species we formed on the polymeric fibers, X-ray diffraction studies were used and the patterns are given in Figure 5. The two strong peaks appearing at 2θ of approximately 19º and 23º are assigned to crystalline polyethylene oxide (Xi et al., 2006). The XRD pattern of the G2 fibers also displays some peaks at 2θ values of 19.9º, 32.6º, 38.0º, and 38.7º, which are related to cobalt hydroxide ($Co(OH)_2$), when compared with the standard XRD data. These peaks are not present in Figure 5b (the product obtained in the electrospinning of a PEO solution having cobalt ions in an air atmosphere, that is, experiment P) and Figure 5c (the product obtained in the electrospinning of pure PEO solution, that is, experiment N). This observation confirms our TEM and TGA result that the $Co(OH)_2$ crystals were formed.

All of the results obtained by the above-mentioned analyses elucidate the reaction ability of traveling polymer jet in electrospinning with an active atmosphere and this

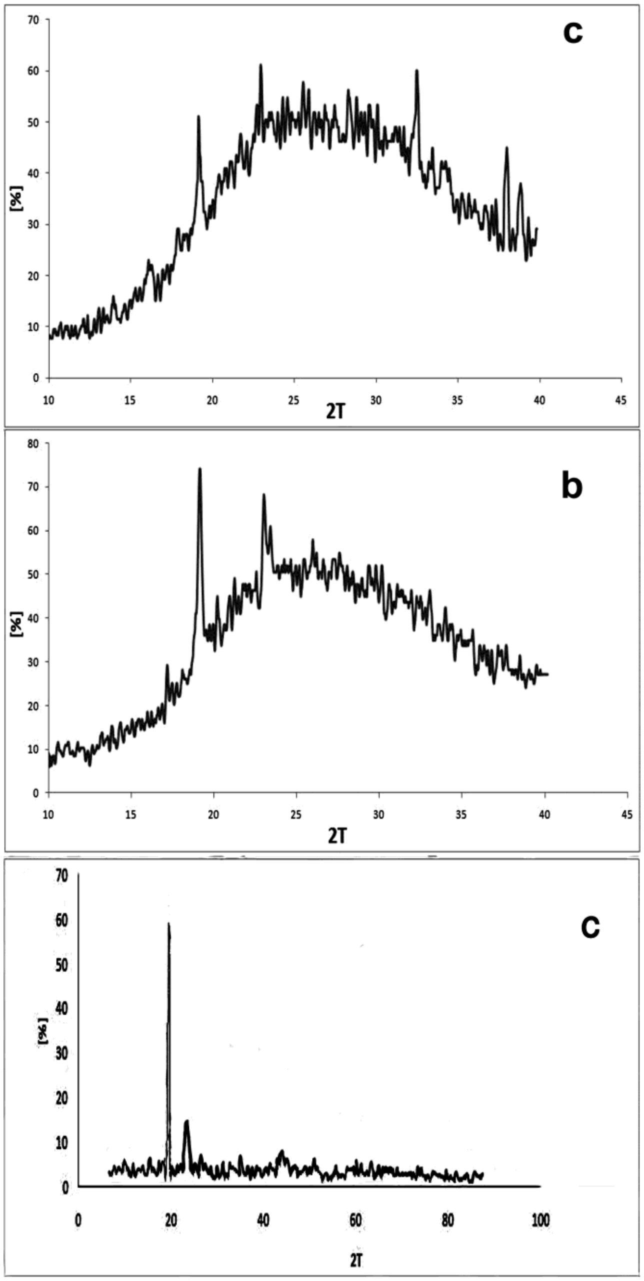

Figure 5: XRD patterns of the nanofiber mats produced in the experiments: G2 (a), P (b), and N (c).

procedure has potential implications in easy production of organic-inorganic hybrid nanofibers and nanostructures.

CONCLUSIONS

Inorganic–polymeric hybrid nanofibers were produced through electrospinning. The nanofibers with 100–600 nm in diameter were produced via occurrence of the reaction of Co^{2+} ions with NH3, which produces $Co(OH)_2$ during electrospinning of PEO solution having Co^{2+} in ammonia atmosphere. The amounts of $Co(OH)_2$ within the fibers decreased with decreases in Co^{2+} concentration in the starting solution. The crystallinity of PEO, shown by DSC analyses, was reduced in electrospinning process in the presence of $Co(OH)_2$ nanoparticles.

ACKNOWLEDGEMENT

The authors wish to acknowledge the financial support provided by the Qatar University via internal grant number

QUST-CENG-SPR-12/13-22.

REFERENCES

Xu ZP, Zeng HC (1999). Interconversion of Brucite-like and Hydrotalcite-like Phases in Cobalt Hydroxide Compounds. Chem. Mater. 11(1): 67-74.

Cao L, Xu F, Liang Y, Li HL (2004). Preparation of the Novel Nanocomposite Co(OH)2/ Ultra-Stable Y Zeolite and Its Application as a Supercapacitor with High Energy Density. Adv. Mater. **16**: 1853.

Zhang L, Dutta AK, Jarero G, Stroeve P (2000). Nucleation and growth of cobalt hydroxide crystallites in organized polymeric multilayers. Langmuir. 16(17): 7095-7100.

Elumalai P, Vasan HN, Munichandraiah N. Electrochemical studies of cobalt hydroxide — an additive for nickel electrodes. J. Power Sources. **93**, 201 (2001).

Srinivasan V, Weidner JW (2002). “Capacitance studies of cobalt oxide films formed via electrochemical precipitation. J. Power Sources. 108(1-2): 15-20.

Barrera E, Gonzalez I, Viveros T (1998). A new cobalt electrodeposit bath for solar absorber. Solar Energy Mater. Solar Cells. 51(1): 69-82.

Kadam LD, Pawar SH, Patil PS (2001). Studies on Ionic Intercalation Properties of Cobalt Oxide Thin Films prepared by spray pyrolysis technique. Mater. Chem. Phys. 68(1-3): 280-282.

Chen GX, Hu ZS, Dong JX, Wang LG, Peng Y, He T, Lai R (2001). "Study on antiwear and reducing friction additive of nanometer cobalt hydroxide". LUBRIC ENG. 57(4): 36-39.

Ramesh TN, Rajamathi M, Kamath PV (2003). “Ammonia induced precipitation of cobalt hydroxide: observation of turbostratic disorder”. Solid State Sci. **5**: 751-756.

Maity A, Biswas MJ (2004). Water-dispersible conducting nanocomposites of binary polymer systems. I. Poly(N-vinylcarbazole)-polyaniline-Al2O3 nanocomposite system. J. Appl. Polym. Sci. **94(2):** 803-811.

Yang QB, Li DM, Hong YL, Li ZY, Wang C, Qiu SL, Wei Y(2003). Preparation and characterization of a pan nanofibre containing Ag nanoparticles via electrospinning. Synth. Met. 137: 973-974.

Yang X, Shao C, Liu Y, Mu R, Guan H (2005). Nanofibers of CeO via an electrospinning technique. Thin Solid Films. **478**(1-2): 228-231.

Lee SW, Kim YU, Choi SS, Park TY, Joo YL, Lee SG (2006). ????????????? PROVIDE TITLE Mater. Lett. **6**1: 889.

Khatri Z, Mayakrishnan G, Hirata Y, Wei K, Kim I (2013). Cationic-cellulose nanofibers: preparation and dyeability with anionic reactive dyes for apparel application Carbohydrate Polymers. **91**(1): 434 -443.

Patnaik P (2002), Handbook of Inorganic Chemicals, McGraw-Hili, New York,

Xi J, Tang X (2004). Nanocomposite polymer electrolyte based on Poly (ethylene oxide) and solid super acid for lithium polymer battery. Chem. Phys. lett. 393(1-3): 271-276.

Xi J, Qiu X, Zhu W, Tang X (2006). Enhanced electrochemical properties of poly(ethylene oxide)-based composite polymer electrolyte with ordered mesoporous materials for lithium polymer battery. Microporous Mesoporous Mater. **88**(1-3): 1-7.